Int. J. Heat Mass Transfer. Vol. 26, No. 1, pp. 41–48, 1983
Printed in Great Britain

0017-9310/83/010041-08 $03.00/0
Pergamon Press Ltd.

BUDGET OF THE TEMPERATURE VARIANCE IN A TURBULENT PLANE JET

R. A. ANTONIA, L. W. B. BROWNE, A. J. CHAMBERS and S. RAJAGOPALAN
Department of Mechanical Engineering, University of Newcastle, N.S.W., 2308, Australia

(*Received* 11 *November* 1981 *and in final form* 1 *June* 1982)

Abstract—Measurements are presented of the advection, production, diffusion and dissipation terms of the mean square temperature fluctuation budget for a two-dimensional jet. Diffusion is more important than advection near the jet centreline. The measured dissipation or destruction, determined using all three components, enables satisfactory closure of the budget in the region of the jet that is free of flow reversal. The difference between the measured dissipation and an estimate, based on local isotropy, is significant across the jet.

NOMENCLATURE

d, nozzle width [m];
f_c, low-pass filter cut-off frequency [Hz];
l_K, Kolmogorov microscale, $(\nu^3/\varepsilon)^{1/4}$ [m];
L_u, half-maximum velocity width [m];
L_θ, half-maximum temperature width [m];
N, average temperature dissipation, equation (2a);
N_i, estimate of N, using local isotropy, equation (2b);
Pe, turbulence Péclet number, $(\overline{u^2})^{1/2}\lambda_\theta/\gamma$;
Pr, molecular Prandtl number, ν/γ;
R_λ, turbulence Reynolds number, $(\overline{u^2})^{1/2}\lambda/\nu$;
T, mean temperature, relative to ambient [°C];
u, velocity fluctuation in x direction [m s^{-1}];
$\overline{uv}$, average kinematic Reynolds shear stress [m^2 s^{-2}];
U, mean velocity in x direction [m s^{-1}];
v, velocity fluctuation in y direction [m s^{-1}];
V, mean velocity in y direction [m s^{-1}];
$\overline{v\theta}$, average thermometric heat flux [m s^{-1} °C];
x, streamwise distance from nozzle [m];
y, distance in direction of shear [m];
z, spanwise direction [m].

Greek symbols

α, coefficient of temperature resistance [°C^{-1}];
γ, thermal diffusivity [m^2 s^{-1}];
ε, average turbulent energy dissipation [m^2 s^{-3}];
η, y/L_u;
η_θ, Corrsin microscale, $(\gamma^3/\varepsilon)^{1/4}$ or $l_K/Pr^{3/4}$ [m];
θ, temperature fluctuation [°C];
λ, Taylor microscale, $[\overline{u^2}/\overline{(\partial u/\partial x)^2}]^{1/2}$ [m];
λ_θ, microscale, $[\overline{\theta^2}/\overline{(\partial\theta/\partial x)^2}]^{1/2}$ [m];
ν, kinematic viscosity [m^2 s^{-1}].

Subscripts

j, refers to conditions at nozzle exit;
0, refers to values on centreline.

1. INTRODUCTION

THE EQUATION for the temperature variance $\overline{\theta^2}$ in a 2-dim. turbulent flow [1] can be simplified, using the boundary layer approximation, to

$$\underbrace{U\frac{\partial\overline{\theta^2}/2}{\partial x}+V\frac{\partial\overline{\theta^2}/2}{\partial y}}_{\text{advection}}+\underbrace{\overline{v\theta}\frac{\partial T}{\partial y}}_{\text{production}}+\underbrace{\frac{1}{2}\frac{\partial\overline{v\theta^2}}{\partial y}}_{\text{diffusion}}+\underbrace{N}_{\text{dissipation}}=0 \quad (1)$$

if the diffusion by heat conduction is ignored. Measurements of terms in equation (1) have been made in several 2-dim. shear flows, including boundary layers and free shear layers. A discussion of the models proposed for various terms in equation (1) is given by Launder [2], who notes that the details of equation (1) in free shear flows depend on the particular flow under investigation. The measurements by Freymuth and Uberoi [3] in the turbulent wake of a heated cylinder indicate that, over a significant part of the wake cross-section, production and dissipation are fairly prominent with moderate contributions by the advection (or convection) and diffusion terms. On and near the wake centreline, dissipation balances the gain in $\overline{\theta^2}$ due to advection and diffusion. Measurements [4] in the wake of a heated sphere appear to be dominated by advection and dissipation over a significant cross-section of the flow. At or near the wake axis advection and dissipation are approximately in balance, a result which is supported by the measurements of Gibson *et al.* [5] on the axis of the heated wake of a sphere. The measurements by Bashir and Uberoi [6] in a heated plane jet into still air indicated approximate equality of diffusion and advection on the centreline but the sum of these terms was about 36% larger than the dissipation, estimated using local isotropy. Antonia *et al.* [7] reported measurements of the budget of $\overline{\theta^2}$ in a circular jet with an external stream. Near the axis of the

jet, contributions from advection and diffusion were approximately equal and their sum approximately in balance with the dissipation, estimated using local isotropy.

The outer regions of circular and plane jets into still air exhibit flow reversal [8, 9]. In the plane jet, flow reversal is likely to be associated with the large scale motion [9, 10] of the flow. It should also be noted that the flapping of the plane jet, suggested by Goldschmidt and Bradshaw [11], is also characteristic of the large scale motion. Since the large scale motion satisfies Reynolds number similarity, flow reversal should not depend on the Reynolds number. The possibility that flow reversal may be influenced by the presence of a solid boundary at the exit plane of a jet cannot be discounted. Moallemi and Goldschmidt [9] found that changing the inclination of the face plates affected the occurrence of flow reversal, especially at small distances from the nozzle. Their measurements also suggest that flow reversal will not disappear with the removal of these plates.

In the present investigation we focus on the measurement of the terms of equation (1) in a region of a plane jet which is essentially free of flow reversal. In particular, all three components of the dissipation N are measured

$$N = \gamma\left[\overline{\left(\frac{\partial\theta}{\partial x}\right)^2} + \overline{\left(\frac{\partial\theta}{\partial y}\right)^2} + \overline{\left(\frac{\partial\theta}{\partial z}\right)^2}\right]. \quad (2a)$$

N is compared with N_i, estimated by assuming local isotropy, viz.

$$N_i = 3\gamma\overline{\left(\frac{\partial\theta}{\partial x}\right)^2}. \quad (2b)$$

Verification of equation (2b) was provided by Freymuth and Uberoi's [3] measurements in the wake of a cylinder which indicated that, across the wake,

$$\overline{\left(\frac{\partial\theta}{\partial x}\right)^2} \simeq \overline{\left(\frac{\partial\theta}{\partial y}\right)^2} \simeq \overline{\left(\frac{\partial\theta}{\partial z}\right)^2}. \quad (3)$$

Equation (3) is not however supported by measurements in other shear flows [12–14]. Also, the assumption of local isotropy is not supported by statistics of $\partial u/\partial t$, $\partial v/\partial t$ and $\partial w/\partial t$ obtained in a plane jet [15, 16].

2. EXPERIMENTAL ARRANGEMENT

The experimental facility consists of a variable-speed centrifugal squirrel cage blower which supplies air to a settling chamber followed by a vertical nozzle of contraction ratio 20:1. An aluminium face plate (Fig. 1) with a central vertical slot of width d = 12.7 mm (aspect ratio is 20) is fixed at the nozzle exit. Two confining horizontal walls are located at the upper and lower edges of the aluminium plate to help maintain the two-dimensionality of the flow. The jet is heated by 1 kW electrical coil elements located immediately downstream of the blower exit.

All the measurements were made at a nominal jet exit velocity U_j of 9 m s^{-1} and a Reynolds number $R_d \equiv U_j d/\nu$ of about 7550. The jet temperature was maintained at a nominal temperature T_j, relative to ambient, of 25°C. Mean velocity and temperature profiles, using a 5 μm hot wire with a DISA 55M01 constant temperature anemometer and a 0.63 μm cold wire drawing 0.1 mA in a constant current circuit, indicated good two-dimensionality of the mean flow at the nozzle exit and at various values of x/d. At the centre of the nozzle exit plane the RMS longitudinal velocity and RMS temperature were estimated to be about 0.5% of the jet exit velocity and temperature, respectively.

Fluctuating temperatures were measured with cold wires operated at very low overheat as resistance thermometers in constant current circuits. Wollaston (Pt–10% Rh) wires of diameter 0.25 μm and 0.63 μm were used with a direct current supply of 0.05 mA (0.25 μm) or 0.1 mA (0.63 μm). The 0.63 μm wire was used primarily to obtain $\overline{\theta^2}$, $\overline{v\theta}$ and $\overline{v\theta^2}$ while both 0.63 and 0.25 μm wires were used for statistics of the temperature derivative $\partial\theta/\partial t$. The frequency response of the cold wires was determined using the pulsed two-wire technique [17]. Although the frequency response of the 0.63 μm wire was adequate for the measurement of $\overline{(\partial\theta/\partial t)^2}$, the 0.25 μm wire has a higher [18] signal to noise ratio than the 0.63 μm wire. Values of $\overline{(\partial\theta/\partial t)^2}$ obtained with 0.25 μm and 0.63 μm wires were in reasonable agreement over the range $30 < x/d < 60$. Derivatives of θ, in the y or z directions, were obtained with a single pair of parallel wires (0.63 μm) mounted on the same probe with a separation of 0.48 mm. After $\partial\theta/\partial y$ was determined, the probe was rotated through 90° to obtain $\partial\theta/\partial z$. The wires were closely matched in resistance, corresponding to a length of about 0.42 mm. The derivative $\partial\theta/\partial y$ (or $\partial\theta/\partial z$) was scaled from the difference in output voltages of the wires. On the jet centreline, the wire length corresponded to $2.6\,l_K$ at $x/d = 40$ and $2\,l_K$ at $x/d = 70$. The Kolmogorov microscale l_K was estimated from $\overline{(\partial u/\partial t)^2}$ using the isotropic relation $\varepsilon = 15\nu\,U^{-2}\,\overline{(\partial u/\partial t)^2}$.

For the measurement of $\partial\theta/\partial t$, the fluctuating voltage across the cold wire was amplified (typically with a gain of 5000), then filtered with a Krohn-Hite model 3322 low-pass filter (48 dB/octave roll off) before analogue differentiation. The output voltage from the differentiator was passed through a second Krohn-Hite 3322 low-pass filter, of identical frequency and phase characteristics to those of the filter used before differentiation. The cut-off frequencies of both filters were set equal to f_c, which was selected using a procedure similar to that outlined in Antonia *et al.* [8]. It was found that f_c was approximately 90% of the Kolmogorov frequency $U/2\pi l_K$.

The RMS value of $(\partial\theta/\partial t)$ was measured at the output of the second Krohn-Hite filter with a DISA 55D35 RMS meter. For a few runs, θ (at the output of the first Krohn-Hite filter) and $\partial\theta/\partial t$ were digitised, for

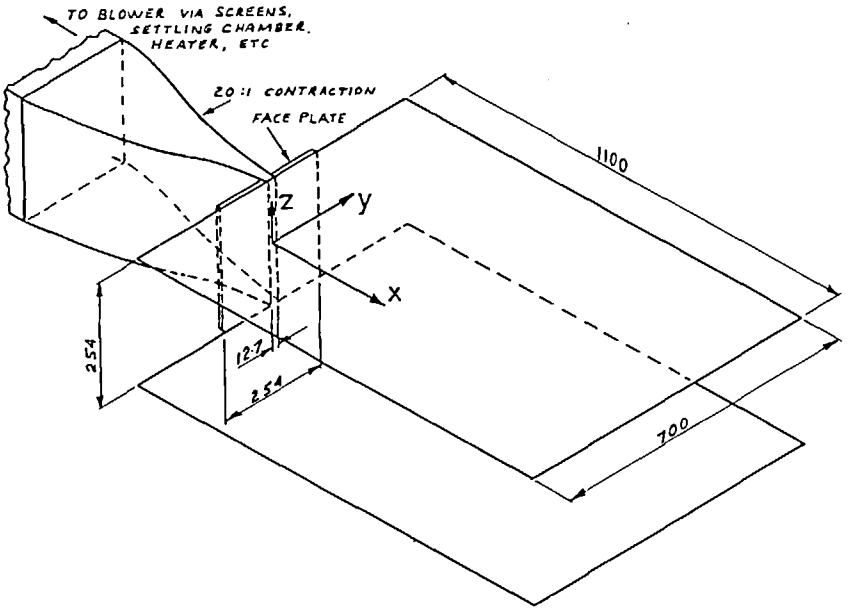

FIG. 1. Schematic diagram (to scale) of plane jet rig. Dimensions are in mm.

a duration of approximately 60 s, using a 12 bit + sign A/D converter, on line to a PDP 11/34 computer. The sampling frequency was set to $2f_c$. Analogue and digital values of $\overline{\theta^2}$ and $\overline{(\partial\theta/\partial t)^2}$ agreed to within 1%.

The temperature coefficient of sensitivity α of the cold wires was measured by mounting the wires at the jet exit plane. The wire resistance was determined by measuring the voltage across the wire (a range of constant currents between 0.05 mA and 0.5 mA were used) over a temperature range extending up to 20°C above the ambient temperature. The resistance values for zero current at these temperatures were found by extrapolation. The mean temperature was measured to an accuracy of ±0.01°C with a 10 Ω Pt resistance thermometer operated with a Leeds & Northrup 8078 temperature bridge. The value of α was found to be $1.69 \times 10^{-3}\,°C^{-1}$ and $1.55 \times 10^{-3}\,°C^{-1}$ for 0.63 μm and 0.25 μm wires respectively.

The velocity fluctuation v was measured with an X-probe with 5 μm Pt–10% Rh Wollaston wires of approximately 0.8 mm length. The wires were mounted in a horizontal plane with a separation of about 0.5 mm. A 0.63 μm cold wire was located 0.5 mm upstream of the centre of the X-probe and perpendicular to the plane of the X-probe. The X-wires were operated with DISA 55M01 constant temperature anemometers at a resistance ratio of 1.8. The X-probe was calibrated for speed and yaw (±25°) at the exit plane of the jet. Signals from the X-probe and cold wire were recorded on an FM tape recorder (Hewlett-Packard 3968A) and subsequently digitised on a PDP 11/34 computer. The temperature contamination of the hot wire signals was first removed before linearising these signals. The velocity contamination of the cold wires was negligible. Signals directly proportional to u, v were obtained after processing the voltages from the hot wires and the cold wires using an analogue computer.

3. MEAN AND RMS VELOCITY AND TEMPERATURE FIELDS

Mean velocity and temperature profiles were measured in the lateral y-direction at several x stations downstream of the nozzle exit extending to 70 nozzle widths. From these traverses, the growth rates for L_u and L_θ were estimated from least squares fits to the data for L_u and L_θ. For $x/d \gtrsim 20$,

$$L_u/d = 0.104\,(x/d + 5) \tag{4}$$

$$L_\theta/d = 0.128\,(x/d + 5), \tag{5}$$

so that $(dL_\theta/dx)/(dL_u/dx)$ is 1.23. For comparison, Davies *et al.* [18] and Jenkins and Goldschmidt [19] obtained ratios of 1.15 and 1.42, respectively. For $x/d \gtrsim 20$, the mean velocity U_0 and mean temperature T_0 decayed according to the following relations

$$\left(\frac{U_j}{U_0}\right)^2 = 0.143\,(x/d + 9) \tag{6}$$

$$\left(\frac{T_j}{T_0}\right)^{1/2} = 0.0115\,(x/d + 110). \tag{7}$$

Distributions of U/U_0 vs η and of T/T_0 vs η were similar for $x/d \geqslant 20$ (Fig. 2). Distributions of $\overline{u^2}^{1/2}/U_0$ vs η and $\overline{\theta^2}^{1/2}/T_0$ vs η were also approximately similar for $x/d \geqslant 20$.

The apparent disparity between virtual origins indicated by the additive terms (inside the brackets) on the RHSs of equations (6) and (7) is of the same order as that inferred from the results of Jenkins and Goldschmidt [20]. These authors obtained slopes of

0.16 and 0.0132 for equations (6) and (7) and additive terms of −4.9 for equation (6) and 85 for equation (7).

4. RESULTS AND DISCUSSION

Equation (1) can be re-written in non-dimensional form by multiplying each term by $L_u/U_0T_0^2$

$$\frac{f}{2}\frac{L_u}{T_0^2}\frac{\partial\overline{\theta^2}}{\partial x}+\frac{k}{2}g'+\frac{\overline{v\theta}}{U_0T_0}h'+\frac{1}{2}\frac{\partial}{\partial\eta}\left(\frac{\overline{v\theta^2}}{U_0T_0^2}\right)+\frac{NL_u}{U_0T_0^2}=0 \quad (8)$$

where a prime denotes differentiation with respect to η. The following similarity distributions for U, V, T and $\overline{\theta^2}$ are assumed (valid for $x/d \gtrsim 20$)

$$\left.\begin{aligned} U &= U_0 f(\eta)\\ V &= U_0 k(\eta)\\ T &= T_0 h(\eta)\\ \overline{\theta^2} &= T_0^2 g(\eta)\end{aligned}\right\} \quad (9)$$

The functions f, g and h were obtained (Fig. 2) using cubic spline least squares fits (implemented on a digital computer) to the experimental data, for U/U_0, $\overline{\theta^2}/T_0^2$ and T/T_0 at $x/d = 40$. The derivatives g' and h' were determined by numerically differentiating the fits for g and h and subsequently applying least squares fits to the estimates for the derivatives. The normal velocity V was calculated, using the continuity equation

$$k = -\frac{L_u}{U_0}\frac{dU_0}{dx}\int_0^\eta f\,d\eta + \frac{dL_u}{dx}\int_0^\eta f'\eta\,d\eta$$

and the derivatives dU_0/dx, dL_u/dx, dT_0/dx (required to estimate $\partial\overline{\theta^2}/\partial x$) were obtained using equations (6), (5) and (7) respectively. The thermometric flux $\overline{v\theta}$ was obtained directly from measurements with the X-probe/cold wire combination, as was the product $\overline{v\theta^2}$ shown in Fig. 3. The diffusion term in equation (8) was determined by first differentiating the least squares fit to the measured values in Fig. 3 and subsequently fitting a least squares curve to the derivative estimates. In Fig. 3, the diffusion curve is not shown beyond $\eta \simeq 1.4$ since values of $\overline{v\theta^2}$ (and, to a lesser extent, $\overline{v\theta}$) become significantly affected by flow reversal in this region of the flow. Flow reversal in the present flow is first detected (the occurrence frequency is very small) at $\eta \simeq 1.0$. This location is approximately independent of x/d (the range investigated here is $20 < x/d < 70$), lending weight to the suggestion [9] that reversal is best interpreted as a characteristic feature of the large scale structure. The detection of flow reversal is identified with the appearance of "spikes" [8] on the signal from the cold wire located 0.5 mm upstream of the centre of the X-wire. When reversal occurs, the thermal wakes from the hot wires contaminate the cold wire signal, the average intensity and frequency of contamination increasing as η increases. Antonia *et al.* [21] found that, in a circular jet, the mean temperature was overestimated by about 16% at the half-temperature radius and they presented measurements of the duration and frequency of occurrence of the reverse flow regions. Similar measurements for a plane jet were obtained by Moallemi and Goldschmidt [9]. No attempt is made here to correct the measurements for flow reversal but the accuracy of the present measurements is expected to impair for $\eta \gtrsim 1.2$. It is possible that improved accuracy in this flow region can be obtained with different measurement techniques, such as the use of pulsed hot-wire or laser anemometers.

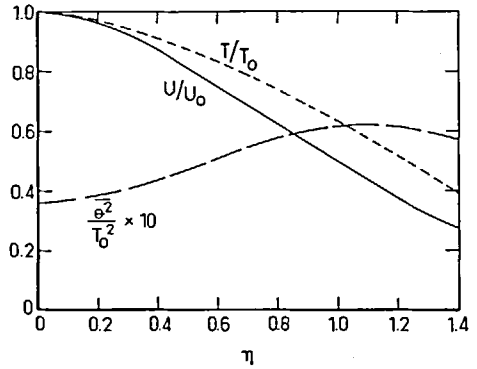

FIG. 2. Mean velocity, mean temperature and RMS temperature distributions at $x/d = 40$. —, U/U_0; ——, T/T_0; – – –, $\overline{\theta^2}/T_0^2 \times 10$. Curves are cubic spline least squares fits to the experimental data.

The budget of $\overline{\theta^2}/2$ is shown in Fig. 4. Advection by the U component of velocity is always significantly larger than that by the V component when $\eta < 1$. The contribution by V becomes more important for $\eta > 1$. The sum of the first two terms in equation (8), plotted in Fig. 4, represents a gain of $\overline{\theta^2}$ for the range of η shown. The magnitude of the turbulent diffusion is significant near the centreline of the jet. The sign of the diffusion of this region is negative so that the diffusion represents a gain of $\overline{\theta^2}/2$. This gain is larger, by nearly a factor of 3, than that due to advection. The diffusion changes sign at $\eta \simeq 0.5$ and represents a loss of $\overline{\theta^2}/2$ for $\eta > 0.5$. The dissipation inferred by difference is, unlike the production, approximately constant in the region $0 < \eta < 1$. The magnitude of this dissipation is in satisfactory agreement with the measured dissipation, obtained with equation (2a), at least for η extending up to about 1.2. For $\eta \gtrsim 1.2$, Fig. 4 suggests that there may be an increase in the imbalance but such an increase may reflect the increasing inaccuracy of the measurements in the reverse flow region.

In view of the reasonable closure of the budget for $\eta \lesssim 1.2$, a comparison between values of N and N_i seems relevant. Estimates of N_i, obtained using equation (2b)*, are shown in Fig. 5. Measurements of $\partial\theta/\partial y$ and

* Taylor's hypothesis was used to convert the time derivative to a streamwise derivative.

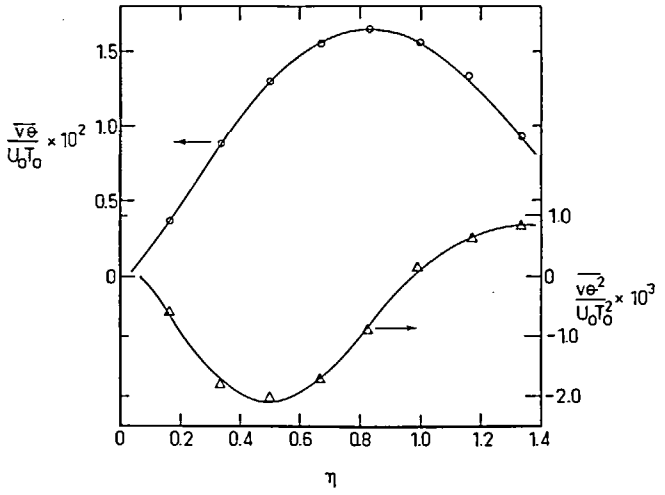

FIG. 3. Distributions of $\overline{v\theta}/U_0T_0$ and $\overline{v\theta^2}/U_0T_0^2$ at $x/d = 40$. ○, $(\overline{v\theta}/U_0T_0 \times 10^2)$; △, $(\overline{v\theta^2}/U_0T_0^2 \times 10^3)$. Curves are cubic spline least squares fits to the experimental data.

$\partial\theta/\partial z$, using the parallel wire probe, indicated that

$$\overline{\left(\frac{\partial\theta}{\partial y}\right)^2} \simeq \overline{\left(\frac{\partial\theta}{\partial z}\right)^2}$$

so that

$$\frac{N}{N_i} = \frac{1}{3}\left[1 + 2\frac{\overline{(\partial\theta/\partial y)^2}}{\overline{(\partial\theta/\partial x)^2}}\right].$$

This ratio is almost 1.5 at $\eta = 0$ and is approximately independent of x/d over the range $30 < x/d < 60$. The magnitude of N/N_i represents a significant departure from local isotropy. While the present results for N/N_i contrast with those of Freymuth and Uberoi [3] for a cylinder wake, they are qualitatively consistent with the ratio N/N_i inferred from Bashir and Uberoi's [6] plane jet measurements. In their case, N was taken to be equal to the imbalance of the $\overline{\theta^2}$ budget and the ratio N/N_i was equal to about 1.36 at $\eta = 0$. The present values of N/N_i are also consistent with those [12, 13] in a boundary layer and in a quasi-homogeneous shear flow [14]. Sreenivasan *et al.* [12] found that $\overline{(\partial\theta/\partial z)^2} > \overline{(\partial\theta/\partial y)^2} > \overline{(\partial\theta/\partial x)^2}$, the average value of $\overline{(\partial\theta/\partial z)^2}/\overline{(\partial\theta/\partial x)^2}$ being about 1.5 in the logarithmic region of the boundary layer. Tavoularis and Corrsin [14] found that $\overline{(\partial\theta/\partial z)^2}/\overline{(\partial\theta/\partial x)^2} \simeq \overline{(\partial\theta/\partial y)^2}/\overline{(\partial\theta/\partial x)^2}$ the ratio being equal to about 1.8.

The possibility of a genuine departure of the fine structure from local isotropy, caused by insufficiently large Reynolds and Péclet numbers should be considered. In the present experiment, the turbulence Reynolds number R_λ, based on the Taylor microscale λ, increases from about 210 at $x/d = 40$ to about 230 at $x/d = 70$ on the jet centreline. The turbulence Péclet number Pe, based on the microscale λ_θ, increases from 100 to 120 over the same x/d range. The present ratio $Pe/R_\lambda \simeq 0.5$ is comparable to that obtained in other shear flows. Tavoularis and Corrsin [14] obtained a value of 0.45 in a quasi-homogeneous shear flow. Values in the range 0.4–0.5 were obtained by Elena [22] and Fulachier [23] in turbulent pipe and boundary layer flows respectively. The present values of R_λ and Pe are perhaps sufficiently large for the existence of an inertial subrange in spectra of u and θ (present spectra confirm this existence approximately half a decade in frequencies). They may not be sufficiently

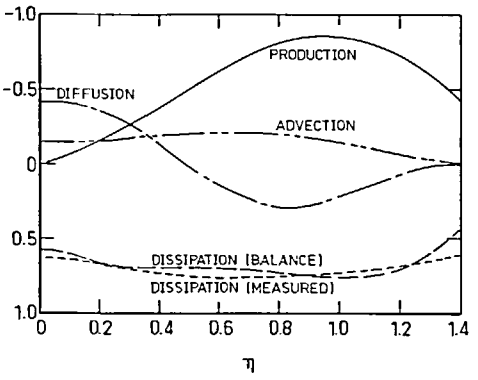

FIG. 4. Measured budget of $\overline{\theta^2}/2$ at $x/d = 40$. —, production, $(\overline{v\theta}/U_0T_0) \times 10^3$; ——, dissipation, $(NL_w/U_0T_0^2) \times 10^3$, by balance; — — —, diffusion, $\frac{1}{2}\partial/\partial\eta\,(\overline{v\theta^2}/U_0T_0^2) \times 10^3$; — · — · —, advection, $[(fL_w/2T_0^2)\partial\overline{\theta^2}/\partial x + kg'/2] \times 10^3$; - - -, measured dissipation.

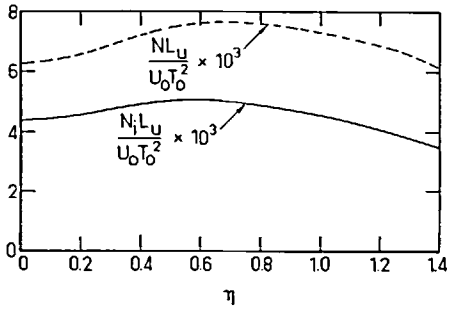

FIG. 5. Dissipation of temperature fluctuations at $x/d = 40$. —, $N_iL_w/U_0T_0^2 \times 10^3$; - - -, $NL_w/U_0T_0^2 \times 10^3$.

large for local isotropy of the temperature and velocity fields.

Support for the apparent breakdown in local isotropy, reflected in the statistics of temperature derivatives, can be found in measurements of the derivatives of all three velocity components. Gutmark and Wygnanski [15] found that, on the centreline of a 2-dim. jet, $\overline{(\partial u/\partial x)^2} \simeq \overline{(\partial w/\partial x)^2}$, while the ratio $\overline{(\partial v/\partial x)^2}/\overline{(\partial u/\partial x)^2}$ decreased slowly with increasing x. Typical values for this ratio were 1.73 at $x/d = 40$ and 1.47 at $x/d = 70$, in contrast with a value of 2 for local isotropy. Everitt and Robins [16] obtained a value of about 1.5 on the centreline of a plane jet into still air. A few measurements of $\overline{(\partial u/\partial x)^2}$, $\overline{(\partial v/\partial x)^2}$ were made in the present study at $x/d = 40$. The magnitude of $\overline{(\partial v/\partial x)^2}/\overline{(\partial u/\partial x)^2}$ was approximately 1.5 on the centreline, and decreased to about 0.6 at $\eta \simeq 1.0$. The expected deviation from local isotropy away from the centreline has also been noted by Gutmark and Wygnanski [15] and Everitt and Robins [16].

It seems pertinent to appraise the accuracy of the important terms in the budget. In particular, meaningful estimates of the accuracy of the dissipation can only be made vis-à-vis an appraisal of the production and diffusion terms in the budget. The uncertainty in $\overline{v\theta}$ was estimated to be $\pm 7\%$ while the uncertainty in determining the production term was estimated to be $\pm 9\%$. It is worth noting that the measured distribution of $\overline{v\theta}$ was in reasonable agreement with the distribution which is calculated from the mean temperature transport equation using the self-preserving forms for the mean velocity and mean temperature. The diffusion term, which involves the gradient of a third order moment, is estimated to have an uncertainty of $\pm 12\%$. A list of possible sources of error in obtaining N, not necessarily in order of importance, is given below:

(1) The effect of the finite separation Δy or Δz for the parallel cold wires on $\overline{(\partial\theta/\partial y)^2}$ and $\overline{(\partial\theta/\partial z)^2}$.

(2) The failure of Taylor's hypothesis due to the fact that the convection velocity is not steady but fluctuates [24, 25].

(3) The likely attenuation of the high frequency end of the derivative spectra due to the finite length of the wires.

(4) The possible effect of unequal time constants of parallel cold wires [14, 26].

Experimental estimates of the effect of Δy on moments of $\partial\theta/\partial y$ were obtained by Sreenivasan *et al.* [12] for a boundary layer. Linear extrapolation of these results to $\Delta y = 0$ suggests that for the present experiment ($\Delta y/l_x \simeq 3$ or $\Delta y/\eta_\theta \simeq 2.4$, with $\eta_\theta \simeq 0.20$ mm at $x/d = 40$), the RMS values of $\partial\theta/\partial y$ and $\partial\theta/\partial z$ could be underestimated by about 14% and N could be underestimated by about 21%. However, the relevance of the boundary layer estimate to the present flow would require verification.

The effect of a fluctuating convection velocity on Taylor's hypothesis, with specific reference to the variance of the temperature derivative can be estimated [25, 27] using certain simplifying assumptions as follows:

$$\overline{\left(\frac{\partial\theta}{\partial x}\right)^2} = \frac{1}{U^2}\overline{\left(\frac{\partial\theta}{\partial t}\right)^2}\left(1 + \frac{\overline{u^2}}{U^2} + \frac{\overline{v^2}}{U^2} + \frac{\overline{w^2}}{U^2}\right)^{-1}. \tag{10}$$

On the centreline of the jet, this expression indicates that the present values of $\overline{(\partial\theta/\partial x)^2}$ could be overestimated by about 13% as a result of using Taylor's hypothesis. Antonia *et al.* [28] showed that when $(U + u)$ is assumed to be the appropriate convection velocity, the value of $\overline{(\partial\theta/\partial t)^2}$ can, in fact, be larger than that given by $U^{-2}\overline{(\partial\theta/\partial t)^2}$. It is not clear, in view of the assumptions made to obtain equation (10) and of the appropriateness of $(U + u)$ as the convection velocity of the fine structure, just precisely what correction should be applied to the data to account for the effect of the second type of error.

While the effect of a finite wire length will cause an attenuation of the high frequency end of the spectrum of the spatial temperature derivative, the magnitude of the attenuation is not known precisely. Wyngaard [29] evaluated numerically the effect of sensor length on the 1-dim. temperature spectrum and on N assuming isotropy and a particular form of the 3-dim. temperature spectrum. If Wyngaard's estimate is assumed to provide a rough indication of the attenuation, N may be underestimated by about 18% in the present experiment.

Possible errors resulting from unequal time constants of the cold wires in the parallel probe arrangement were discussed by Mestayer and Chambaud [26]. Corrections for this effect were not applied to the present data as the cold wire signals were filtered at the same value of f_c and the measured "-3 dB" frequencies of the cold wires were larger than f_c.

Whilst the overall effect of the four sources of error listed above cannot be regarded as conclusive (clearly more work is required on the first three), it seems unlikely that this effect would be such as to account for the systematic difference reported in Fig. 5, between N and N_i. The encouraging agreement between the measured values of N and those obtained from the imbalance of the budget and the discrepancy between N and N_i indicated by Bashir and Uberoi's [6] measurements seem to rule out the use of equation (2b) for measuring the dissipation in this flow.

Acknowledgements—The authors would like to thank Mr. M. J. Watts for assisting with preliminary measurements. The support of the Australian Research Grants Committee is gratefully acknowledged.

REFERENCES

1. S. Corrsin, Heat transfer in isotropic turbulence, *J. Appl. Phys.* **23**, 113–118 (1952).

2. B. E. Launder, Heat and mass transport, in *Turbulence—Topics in Applied Physics* (edited by P. Bradshaw) Vol. 12, pp. 231–287. Springer (1978).
3. P. Freymuth and M. S. Uberoi, Structure of temperature fluctuations in the turbulent wake behind a heated cylinder, *Phys. Fluids* **14**, 2574–2580 (1971).
4. P. Freymuth and M. S. Uberoi, Temperature fluctuations in the turbulent wake behind an optically heated sphere, *Phys. Fluids* **16**, 161–168 (1973).
5. C. H. Gibson, C. C. Chen and S. C. Lin, Measurements of turbulent velocity and temperature fluctuations in the wake of a sphere, *AIAA Jl.* **6**, 642–649 (1968).
6. J. Bashir and M. S. Uberoi, Experiments on turbulent structure and heat transfer in a two-dimensional jet, *Phys. Fluids* **18**, 405–410 (1975).
7. R. A. Antonia, A. Prabhu and S. E. Stephenson, Conditionally sampled measurements in a heated turbulent jet, *J. Fluid Mech.* **72**, 455–480 (1975).
8. R. A. Antonia, B. R. Satyaprakash and A. K. M. F. Hussain, Measurements of dissipation rate and some other characteristics of turbulent plane and circular jets, *Phys. Fluids* **23**, 695–700 (1980).
9. M. K. Moallemi and V. W. Goldschmidt, Smoke wire visualization of the external region of a two-dimensional jet, *Proc. 7th Biennial Symp. on Turbulence*, University of Missouri-Rolla, paper 42 (1981).
10. J. W. Oler and V. W. Goldschmidt, Coherent structures in the similarity region of two-dimensional turbulent jets, *Proc. 3rd Symp. on Turbulent Shear Flows*, University of California at Davis, 11.1–11.6 (1981).
11. V. W. Goldschmidt and P. Bradshaw, Flapping of a plane jet, *Phys. Fluids* **16**, 354–355 (1973).
12. K. R. Sreenivasan, R. A. Antonia and H. Q. Danh, Temperature dissipation fluctuations in a turbulent boundary layer, *Phys. Fluids* **20**, 1238–1249 (1977).
13. R. A. Antonia, A. J. Chambers, D. Phong-Anant and S. Rajagopalan, Properties of spatial temperature derivatives in the atmospheric surface layer, *Bound.-Layer Meteorol.* **17**, 101–118 (1979).
14. S. Tavoularis and S. Corrsin, Experiments in nearly homogeneous turbulent shear flow with a uniform mean temperature gradient. Part 2. The fine structure, *J. Fluid Mech.* **104**, 349–367 (1981).
15. E. Gutmark and I. Wygnanski, The planar turbulent jet, *J. Fluid Mech.* **73**, 465–495 (1976).
16. K. W. Everitt and A. G. Robins, The development and structure of turbulent plane jets, *J. Fluid Mech.* **88**, 563–583 (1978).
17. R. A. Antonia, L. W. B. Browne and A. J. Chambers, Determination of time constant of cold wires, *Rev. Scient. Instrum.* **52**, 107–110 (1981).
18. R. A. Antonia, L. W. B. Browne and A. J. Chambers, Use of fine cold wires for the measurement of dissipation of temperature fluctuations, *DISA Information* No. 27, 27–30 (1982).
19. A. E. Davies, J. F. Keffer and D. W. Baines, Spread of a heated plane turbulent jet, *Phys. Fluids* **18**, 770–775 (1975).
20. P. E. Jenkins and V. W. Goldschmidt, Mean temperature and velocity in a plane turbulent jet, *J. Fluids Engng* **95**, 581–584 (1973).
21. R. A. Antonia, A. J. Chambers and A. K. M. F. Hussain, Errors in simultaneous measurements of temperature and velocity in the outer part of a heated jet, *Phys. Fluids* **23**, 871–874 (1980).
22. M. Elena, Etude expérimentale de la turbulence au voisinage de la paroi d'un tube légérement chauffé, *Int. J. Heat Mass Transfer* **20**, 935–944 (1977).
23. L. Fulachier, Contribution à l'étude des analogies des champs dynamique et thermique dans une couche limite turbulente. Effet de l'aspiration, Thèse de Doctorat ès Sciences, Université de Provence, Marseille (1972).
24. J. L. Lumley, Interpretation of time spectra measured in high-intensity shear flows, *Phys. Fluids* **8**, 1056–1062 (1965).
25. J. C. Wyngaard and S. F. Clifford, Taylor's hypothesis and high frequency turbulence spectra, *J. Atmos. Sci.* **34**, 992 (1981).
26. P. Mestayer and P. Chambaud, Some limitations to measurements of turbulence microstructure with hot and cold wires, *Bound.-Layer Meteorol.* **16**, 311–329 (1979).
27. F. H. Champagne, C. A. Friehe, J. C. LaRue and J. C. Wyngaard, Flux measurements, flux estimation techniques, and fine-scale turbulence measurements in the unstable surface layer over land, *J. Atmos. Sci.* **34**, 515 (1977).
28. R. A. Antonia, N. Phan-Thien and A. J. Chambers, Taylor's hypothesis and the probability density functions of temporal velocity and temperature derivatives in a turbulent flow, *J. Fluid Mech.* **100**, 193–208 (1980).
29. J. C. Wyngaard, Spatial resolution of a resistance wire temperature sensor, *Phys. Fluids* **14**, 2052–2054 (1971).

BILAN DE LA VARIATION DE TEMPERATURE DANS UN JET PLAN TURBULENT

Résumé—On présente des mesures des termes de transport, production, diffusion et de dissipation des valeurs efficaces des fluctuations de température pour un jet bidimensionnel. La diffusion est plus importante que l'advection près de la ligne des centres. La dissipation ou la destruction mesurée, déterminée à partir des trois composantes, fournit une fermeture satisfaisante du bilan dans la région du jet qui ne compte pas d'écoulement de retour. La différence entre la dissipation mesurée et celle estimée, basée sur l'isotropie locale est sensible à travers le jet.

DIE GESAMTHEIT DER TEMPERATURVARIANZ IN EINEM TURBULENTEN EBENEN STRAHL

Zusammenfassung—Es wird über Messungen der Advektions-, Produktions-, Diffusions- und Dissipationsterme des quadratischen Mittelwerts der Gesamtheit der Temperaturschwankungen in einem zweidimensionalen Strahl berichtet. Die Diffusion ist in der Nähe des Strahlungskernes von größerer Bedeutung als die Advektion. Die gemessene Dissipation oder Destruktion, die unter Berücksichtigung aller drei Komponenten bestimmt wurde, ermöglicht eine zufriedenstellende Formulierung der Gesamtheit der Temperaturvarianz im rückströmungsfreien Bereich des Strahls. Die Differenz zwischen der gemessenen Dissipation und der auf der Grundlage örtlicher Isotropie berechneten ist im gesamten Strahl gravierend.

БАЛАНС ПУЛЬСАЦИЙ ТЕМПЕРАТУРЫ В ТУРБУЛЕНТНОЙ ПЛОСКОЙ СТРУЕ

Аннотация—Представлены результаты измерения различных членов в уравнении баланса пульсаций температуры, конвекции, порождения, диффузии и диссипации для неизотермического течения в плоской струе. В центре струи диффузия вносит более существенный вклад, чем конвекция. Измерение диссипации (или деструкции) пульсаций температуры, для определения которой используются все три компоненты, позволяет получить удовлетворительный баланс в области струи, свободной от возвратных течений. Различие между измеренными значениями диссипации и оценками, полученными на основе локальной изотропии, оказывается существенным по всему сечению струи.